

Photon migration in non-scattering tissue and the effects on image reconstruction

H Dehghani[†], D T Delpy[†] and S R Arridge[‡]

[†] Department of Medical Physics and Bioengineering, University College London, 11–20 Capper Street, London WC1E 6JA, UK

[‡] Department of Computer Science, University College London, Gower Street, London WC1E 6BT, UK

Received 26 April 1999, in final form 23 August 1999

Abstract. Photon propagation in tissue can be calculated using the relationship described by the transport equation. For scattering tissue this relationship is often simplified and expressed in terms of the diffusion approximation. This approximation, however, is not valid for non-scattering regions, for example cerebrospinal fluid (CSF) below the skull. This study looks at the effects of a thin clear layer in a simple model representing the head and examines its effect on image reconstruction. Specifically, boundary photon intensities (total number of photons exiting at a point on the boundary due to a source input at another point on the boundary) are calculated using the transport equation and compared with data calculated using the diffusion approximation for both non-scattering and scattering regions. The effect of non-scattering regions on the calculated boundary photon intensities is presented together with the advantages and restrictions of the transport code used. Reconstructed images are then presented where the forward problem is solved using the transport equation for a simple two-dimensional system containing a non-scattering ring and the inverse problem is solved using the diffusion approximation to the transport equation.

1. Introduction

Optical tomography involves the non-invasive and non-hazardous measurement of photon flight through biological tissue. These measurements can be used to obtain information about anatomical structure as well as the physiological state of the tissue under investigation. The optical properties of tissue vary considerably over a range of wavelengths. The characteristic tissue scatter is commonly expressed in terms of the transport scatter coefficient (the probability of a photon scattering in a given distance), $\mu'_s = \mu_s(1 - g)$, where g is the mean cosine of the single scatter function (the anisotropy factor) and μ_s is the scatter coefficient. At a wavelength of 800 nm, μ'_s is typically about 1–2 mm⁻¹ for breast and neonatal brain tissue and larger for muscle and adult brain. The other major optical property of concern is the absorption coefficient, μ_a , which at a wavelength of 800 nm is approximately 0.01–0.025 mm⁻¹ for soft tissue but generally increases with wavelength since the dominant component in most soft tissue is water. However, very strong absorption from haemoglobin in blood at wavelengths less than 650 nm limits the wavelength range of the radiation that can be used for imaging through several centimetres of tissue to the red and near-infrared (NIR) region (Hebden *et al* 1997).

Numerical modelling of light propagation in scattering tissue has become well established in optical tomography (Arridge *et al* 1993, Arridge 1999, Schweiger *et al* 1995) largely through the use of the diffusion approximation to the transport equation. The diffusion approximation

is only valid for materials that are much more scattering than absorbing. This is acceptable at appropriate wavelengths (650–900 nm) where biological tissues have a μ'_s that is much larger than μ_a , for instance in breast tissue. There has therefore been considerable work on imaging of the breast (Colak *et al* 1997, Fantini *et al* 1996) using photons measured on the surface of the tissue to enable the detection and perhaps characterization of abnormalities within the tissue. Our major interest in optical tomography, however, lies in its use for the imaging of the neonatal head. In such studies the aim would be to detect changes in the oxygenation state of specific regions of the brain as an aid to the understanding and prevention of cerebral handicap. Within the head, however, there are regions which are non-scattering while still absorbing, namely the CSF layer around the brain and in the ventricles. The presence of CSF prevents the accurate modelling of photon propagation within the regions of interest when using the diffusion approximation. Despite this, many groups have developed diffusion-based image reconstruction algorithms on the assumption that the error introduced by this approximation may be small or clinically acceptable (Schweiger *et al* 1993, Jiang *et al* 1995, Pogue *et al* 1995).

A small number of studies have been performed to investigate the accuracy of the diffusion approximation in regions where μ_a is larger than μ'_s (Hielscher and Alcouffe 1996, Nakai *et al* 1997, Bassani *et al* 1997). Hielscher and Alcouffe have found that when μ_a is comparable to μ'_s , the results calculated using the diffusion approximation differ significantly from those of the transport equation. To ensure small differences between the transport theory and the diffusion approximation, these researchers further state that the μ'_s/μ_a ratio needs to be no less than 40:1, whereas Nakai *et al* (1997) and Bassani *et al* (1997) state this ratio to be as low as 3:1. There is therefore a need for accurate information on the way photon propagation and density vary with tissue distribution in a model approximating the neonatal head, where μ_a and μ'_s may vary unconditionally.

Previous studies using numerical modelling and experimental results have shown the effect of clear layers on the system measurements (Firbank *et al* 1996, Okada *et al* 1997, Wang *et al* 1998). All studies report that thin clear non-scattering layers have a significant effect upon light distribution in the system.

In this study we have used two numerical models of photon transport. The first model is a time-independent finite difference transport code, DANTSYS, which was originally developed by Alcouffe *et al* (1995) for neutron transport studies, and second is a diffusion approximation model as discussed by Arridge *et al* (1993) and Schweiger *et al* (1995). DANTSYS has been previously used for simulation of photon transport in the presence of a clear region (Hielscher and Alcouffe 1996, Hielscher *et al* 1997), and for simple geometries comparisons have been made with analytical solutions of the diffusion approximation. The initial part of this work is to examine the accuracy of DANTSYS in simulations of photon propagation in scattering material with the aim of investigating the effect due to the presence of non-scattering media. Finally the validity of using a diffusion-based image reconstruction scheme on data from objects containing clear regions is examined. This involved reconstructing images of μ_a distribution using the diffusion approximation for the solution of the inverse problem, but with photon intensity data calculated using the transport code in the presence of a non-scattering ring of varying thickness.

2. Models of photon transport

Photon propagation is described by the radiative transfer equation (RTE) (Chandrasekhar 1950, Case and Zweifel 1967), which for the single-energy time-dependent case is given as:

$$\left(\frac{1}{c} \frac{\partial}{\partial t} + \hat{s} \cdot \nabla + \mu_{tr}(\mathbf{r})\right) \phi(\mathbf{r}, \hat{s}, t) = \mu_s(\mathbf{r}) \int p(\hat{s} \cdot \hat{s}') \phi(\mathbf{r}, \hat{s}', t) d^2 \hat{s}' + q(\mathbf{r}, \hat{s}, t) \quad (1)$$

where c is the speed of light within the medium, $\mu_{tr}(r)$ is the transport cross section at point r , $\phi(r, \hat{s}, t)$ is the radiance at position r , time t , direction \hat{s} and $q(r, \hat{s}, t)$ is the source. p defines the probability that during a scattering event a photon from direction \hat{s}' is scattered in the direction \hat{s} .

Under the assumption that scattering dominates absorption in a region of interest, the transport equation, equation (1), can be simplified by the use of the diffusion approximation which is obtained by only considering the P1 spherical expansion of equation (1):

$$-\nabla \cdot D(\mathbf{r})\nabla\Phi(\mathbf{r}, t) + \mu_a\Phi(\mathbf{r}, t) + \frac{1}{c} \frac{\partial\Phi(\mathbf{r}, t)}{\partial t} = q_0(\mathbf{r}, t) \quad (2)$$

where $q_0(r, t)$ is the zeroth order for the expansion of $q(r, \hat{s}, t)$ (isotropic source) and $\Phi(r, t)$ is the photon density at position r , time t , and is given by:

$$\Phi(\mathbf{r}, t) = \int \phi(\mathbf{r}, \hat{s}, t) d^2\hat{s}. \quad (3)$$

The diffusion coefficient D is given by:

$$D = \frac{1}{3(\mu_a + \mu'_s)}. \quad (4)$$

For biological tissue the value of g is usually about 0.9 which describes a mainly forward scatter for the tissue. Theoretical and experimental results have so far demonstrated the validity of these equations under appropriate conditions where $\mu'_s \gg \mu_a$ (Groenhuis *et al* 1983, Nakai *et al* 1997, Bassani *et al* 1997).

3. Homogeneous scattering regions

Initially photon flux in a two-dimensional (2D) circular model of radius 25 mm with a homogeneous scatter of $\mu'_s = 2 \text{ mm}^{-1}$ and absorption of $\mu_a = 0.025 \text{ mm}^{-1}$ was solved using three methods:

- (a) An analytical solution based on the diffusion approximation (Arridge *et al* 1992).
- (b) A finite difference model of the RTE, DANTSYS (Alcouffe *et al* 1995).
- (c) A finite element model based on the diffusion approximation (Arridge *et al* 1993, Schweiger *et al* 1995).

The source was modelled as a single isotropic source situated a single transport scattering distance (0.5 mm) inside the boundary. For the DANTSYS model great care was taken to ensure a sufficient number of elements were used to allow accurate modelling (Hielscher *et al* 1996): as a rule of thumb adjacent element nodes should not be separated by more than one transport mean free path $\frac{1}{\mu'_s}$. The value of g was assumed to be zero, so that $\mu'_s = \mu_s$. Boundary photon intensities were hence calculated for all three models for a given point source (figure 1). It can be seen from these results that all three models calculate the same data with similar accuracy. Hielscher and Alcouffe (1996) have also published similar results. The boundary condition used in the transport model is a condition where the angular flux on the boundary is identically zero for all incoming directions (vacuum boundary condition as specified in DANTSYS). It is believed that for the finite element diffusion approximation model, the Robin boundary condition (representing a physical model of a non-scattering medium surrounding the area of interest and assuming that no diffuse surface reflection at the outer boundary occurs) as discussed by Schweiger *et al* (1995) would be most applicable. However, the Dirichlet boundary condition (assuming that the photon density at the boundary is zero) was found to best match the data from the transport model. For the analytical model, a Dirichlet boundary condition was also used.

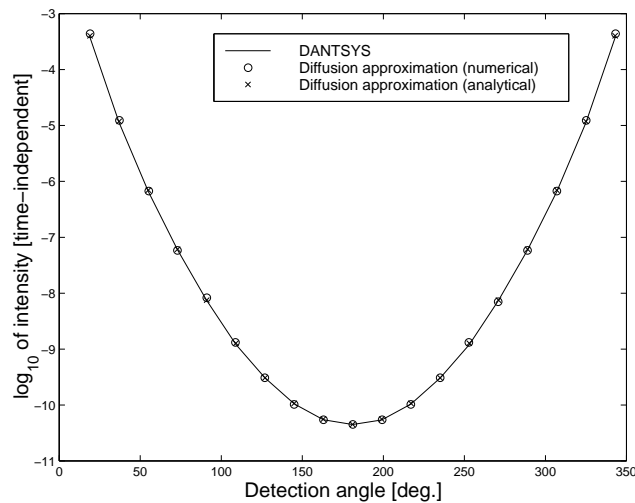


Figure 1. Calculated boundary flux for a circular model of radius 25 mm. $\mu'_s = 2 \text{ mm}^{-1}$ and $\mu_a = 0.025 \text{ mm}^{-1}$ throughout the model. The full curve represents boundary flux calculated using DANTSYS, circular points represent flux calculated using a numerical model of the diffusion approximation and crosses represent the flux calculated using the analytical solution of the diffusion approximation. The detection angle represents the angular position of each measurement point with respect to the source.

4. A clear non-scattering ring within a homogeneous scattering region

The diffusion approximation is known to be invalid in non-scattering regions and it is for this reason that solutions to the transport equation are required for accurate modelling of the head. Methods other than the transport equation have also been proposed and used for systems containing non-scattering regions (Firbank *et al* 1996). In their study, an iterative hybrid radiosity-diffusion model was used to solve for time-dependent solutions for scattering models containing non-scattering regions.

Qualitative studies have already shown the capability of DANTSYS in calculating the photon densities not only in scattering regions but also in non-scattering media (Hielscher *et al* 1997). In the next part of this study a circular model of radius 25 mm was used. This model (figure 2) consists of a homogeneous distribution where $\mu'_s = 2 \text{ mm}^{-1}$ and $\mu_a = 0.025 \text{ mm}^{-1}$ (shaded region) except for a ring of 2 mm thickness at radius 20 mm extending to radius 22 mm (white region). For this clear ring, in the DANTSYS model, $\mu'_s = 0 \text{ mm}^{-1}$ (no scatter) and $\mu_a = 0.025 \text{ mm}^{-1}$ were used and for the diffusion approximation model $\mu'_s = 0.005 \text{ mm}^{-1}$ (very little scatter) and $\mu_a = 0.025 \text{ mm}^{-1}$. The μ_a of the clear ring was given a value of 0.025 mm^{-1} , so that the absorption coefficient throughout the model was kept constant. This ensures that any effects seen are purely due to the non-scattering property of the region. The source was modelled as a single isotropic source situated a single transport scattering distance (0.5 mm) inside the boundary.

In DANTSYS for the discretization of the direction or angles of photon propagation, the discrete ordinate method (also known as the S_n method) is used (Alcouffe *et al* 1995). Carlson and Lathrop (1968) and Dunderstadt and Martin (1979) give a good description of this method. In order to ensure that an adequate number of discrete ordinates (variable S_n , as defined in DANTSYS) are used, a number of simulations were performed for various values of S_n . It was found that no significant changes in the calculation of flux densities were seen when S_n

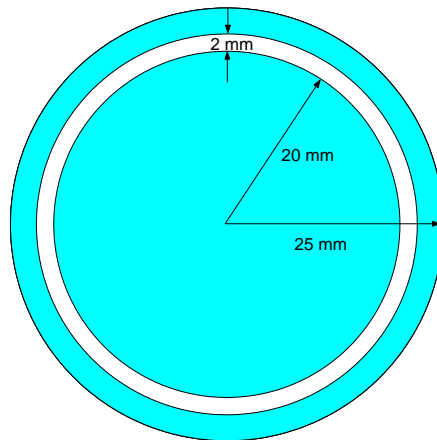


Figure 2. Circular model of radius 25 mm. The shading represents a scattering region where $\mu'_s = 2 \text{ mm}^{-1}$ and $\mu_a = 0.025 \text{ mm}^{-1}$. The white region of thickness 2 mm from radius 20 mm to 22 mm represents a non-scattering region where $\mu'_s = 0 \text{ mm}^{-1}$ and $\mu_a = 0.025 \text{ mm}^{-1}$ in the DANTSYS model and $\mu'_s = 0.005 \text{ mm}^{-1}$ and $\mu_a = 0.025 \text{ mm}^{-1}$ in the diffusion approximation model.

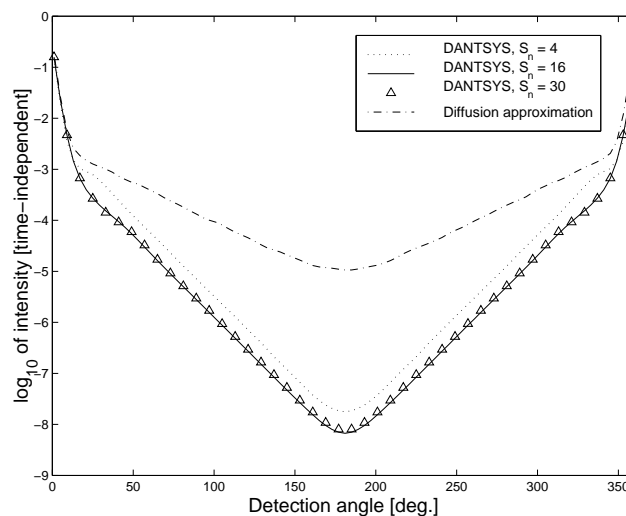


Figure 3. The calculated boundary flux for a circular model as shown in figure 2. Detection angle represents the angular position of each measurement point with respect to the source. S_n values of 4, 16 and 30 correspond to 16, 256 and 900 angular directions respectively.

was greater than 30. It is noted here that for such a large number of discrete ordinates, the calculation time required is increased many fold.

The boundary fluxes calculated for the DANTSYS model (for $S_n = 4, 16$ and 30) and the diffusion approximation model for a given point source are shown in figure 3. It can be seen that the diffusion approximation model clearly overestimates the flux density at the boundary in the presence of the clear layer. The flux calculated using DANTSYS for three values of S_n is shown. It can be seen that for an increase of S_n from 16 to 30, the changes

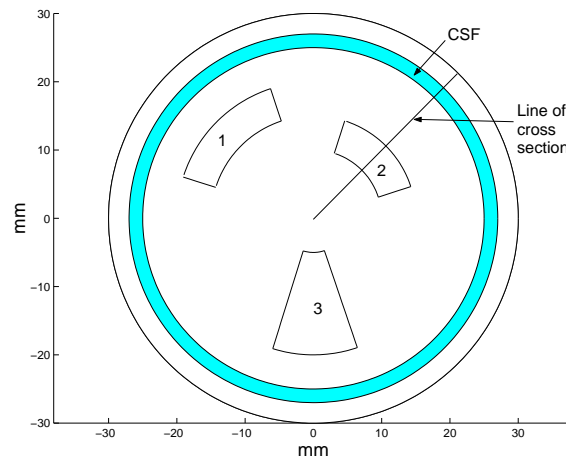


Figure 4. Outline of the model used to calculate boundary flux intensity data for a circular phantom ($\mu'_s = 2 \text{ mm}^{-1}$ and $\mu_a = 0.025 \text{ mm}^{-1}$) of radius 30 mm in the presence of a CSF ring ('void') ($\mu'_s = 0 \text{ mm}^{-1}$ and $\mu_a = 0 \text{ mm}^{-1}$) at radius 27 mm. Three anomalies ($\mu'_s = 2 \text{ mm}^{-1}$ and $\mu_a = 0.05 \text{ mm}^{-1}$) are placed as shown (labelled as 1, 2 and 3).

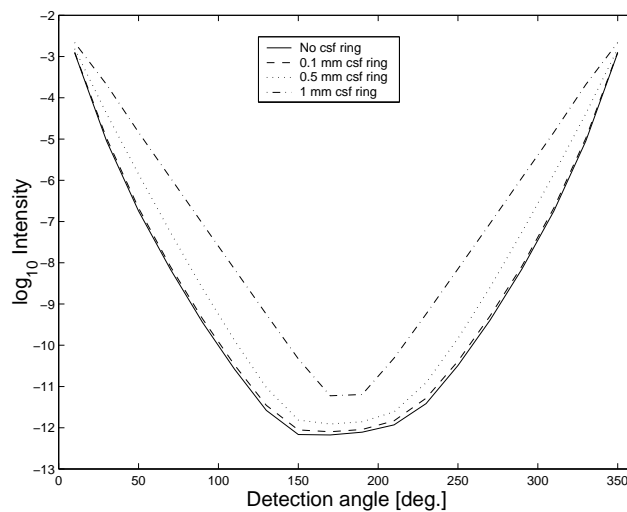


Figure 5. Boundary flux calculated for the model shown in figure 4. The flux is due to one source point and is calculated when no CSF ring is modelled as well as in the presence of the CSF ring where its thickness varies from 0.1 mm to 1 mm. Flux calculated at measurement points are only shown, between angles of 10° to 350° .

of the boundary flux are small. For an S_n value of 30, the calculation time for a model of a single point source is very long, approximately 12 h on a SUN workstation (266 MHz, 128M RAM). The calculation times for S_n values of 4, 8, 10 and 20 are 15 min, 1 h, 1.5 h and 4.5 h respectively. Similar results (not shown) can be obtained when modelling a thin layer of CSF (1 mm), where the diffusion approximation still overestimates the calculated flux density.

5. Image reconstruction using the diffusion approximation with data calculated in the presence of a clear region

Image reconstruction in optical tomography is well established and has been described in detail by Arridge (1999), Schweiger *et al* (1993), Jiang *et al* (1995) and Pogue *et al* (1995). Usually boundary data (flux intensities, mean time of flight as well as other possible data types) are calculated with a forward model using the diffusion approximation and images of absolute optical properties for the regions of interest are reconstructed. In this part of the study, we attempt to reconstruct images using the diffusion approximation with flux intensity data that have been calculated in a model containing absorption anomalies and a clear region (using DANTSYS). No other data types could be used in this instance as DANTSYS is only capable of producing time-independent flux intensities.

DANTSYS is thought to be able to deal with 'void' regions. By 'void' we mean non-scattering and non-absorbing regions within the model. To allow a void calculation in DANTSYS, the region label '0' was assigned to the void regions (Alcouffe *et al* 1995). A circular model of radius 30 mm, containing a void ring as well as three separate anomalies, was used to calculate the boundary flux intensity data using DANTSYS (figure 4). The thickness of the clear ring, which was positioned at 27 mm from the centre of the model, was varied from 0.1 mm to 0.5 mm and 1 mm with a void property. The anomalies were of equal scattering to the rest of the model with $\mu'_s = 2 \text{ mm}^{-1}$ but had twice the background absorption with $\mu_a = 0.05 \text{ mm}^{-1}$. Boundary flux intensities were calculated at 18 equidistant points on the boundary for 18 separate equidistant sources placed at one transport scattering depth inside the outer boundary.

The calculated boundary data for a single source point are shown in figure 5. It is evident that even in the presence of a 0.1 mm CSF ring the boundary flux is slightly affected compared with that when no CSF ring is present. Also as the thickness of the CSF ring increases, the number of photons propagating through the medium increases, which is as expected. Furthermore it is evident from these data that even when the CSF ring is only 1 mm thick, a high proportion of photons detected at the surface have travelled through the clear ring giving rise to the regions of linear flat response as seen in figure 5.

Images of the absorption coefficient were reconstructed using a nonlinear conjugate-gradient image reconstruction method (Arridge and Schweiger 1998) with median filtering at each iteration. One hundred iteration steps were used and the reconstructed images for each case at one hundredth iteration step is shown in figure 6. It was found that for the purpose of image reconstruction, the diffusion model with a Robin boundary condition produced more accurate images than those with a Dirichlet boundary condition.

Several features of these images are apparent. The first is that in the presence of a very thin clear layer the diffusion approximation is still able to reconstruct images of the absorption coefficient distribution. However, as the thickness of this clear layer is increased, the quality of the reconstructed images decreases. For the case where the clear layer is 1 mm thick, it is found that the three separate anomalies are not distinguishable. A notable feature is that as the thickness of the clear layer is increased, the anomalies are reconstructed slightly displaced from their original position. Figure 7 shows a plot of the calculated μ_a along the line of intersection as shown in figure 4. It is noted that as the thickness of the clear layer increases, the anomaly appears to be moving slightly closer towards the boundary of the model. Furthermore it is evident that for a CSF ring of 1 mm the calculated μ_a is highly inaccurate.

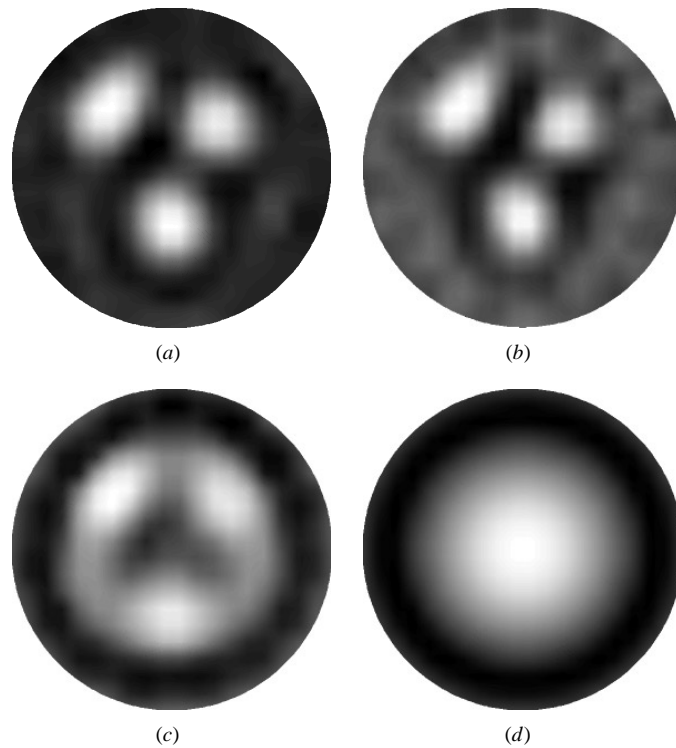


Figure 6. Top left (a): μ_a images reconstructed with the diffusion model using the conjugate gradient method (100 iterations) for the data calculated using the diffusion approximation in the presence of no clear layer. Top right and bottom row (b)–(d): μ_a images reconstructed with the diffusion model (conjugate gradient method, 100 iterations) with data calculated using DANTSYS in the presence of a non-scattering ring of thickness (b) 0.1 mm, (c) 0.5 mm and (d) 1 mm.

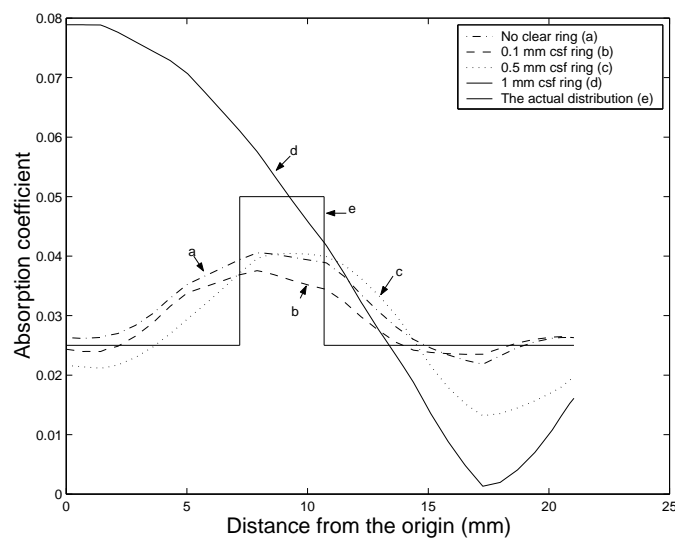


Figure 7. Calculated μ_a along a line of cross section (figure 4) for each of the reconstructed images (figure 6) with varying CSF thickness. As the thickness of the CSF ring increases the position of the peak value of μ_a moves out towards the boundary of the CSF ring.

6. Discussions and conclusions

For the accurate imaging of the neonatal head the presence of non-scattering (clear) regions must be taken into account. Numerical modelling of photon propagation is an essential tool in most image reconstruction schemes and must therefore produce accurate results. In the presence of a clear region, the diffusion approximation of photon transport is shown as no longer valid. The calculated boundary flux intensity is highly overestimated when using this approximation. For this reason a transport code for RTE was used to calculate the boundary photon intensity for a circular model of radius 30 mm containing a clear ring and three absorbing anomalies. It has been shown that when the clear ring has a thickness of up to 0.5 mm, the boundary data can still be used for image reconstruction using a diffusion approximation. In the presence of a thin clear ring the reconstructed images of the anomalies appear to be more blurred and slightly displaced away from the centre of circular model and towards the boundary of the clear annular ring. For a clear ring of 1 mm, no useful image can be reconstructed using the diffusion approximation.

The transport code used in this study is a time-independent code and so only flux intensity data were available. It may be that other data types, such as mean time of flight, will produce better results in the presence of a clear region. However, the calculation of such data types using DANTSYS was not possible. The calculation time for a single model using this transport code was approximately 12 h on a relatively fast computer, and clearly the use of this transport code for any iterative image reconstruction scheme is not feasible, although more efficient schemes have been developed (Dorn 1998). However, work is currently under way on the development of an alternative calculation scheme for flux intensities and mean time of flight as well other data types in the presence of clear regions (Arridge *et al* 1999).

References

- Alcouffe R E, Baker R S, Brinkley F W, Marr D R, Dell R D and Walters W F 1995 DANTSYS: a diffusion accelerated neutral particle transport code system *Manual LA-12969-M* (Los Alamos, NM: Los Alamos National Laboratory)
- Arridge S R 1999 Optical tomography in medical imaging *Inverse Problems* **15** R41–R93
- Arridge S R, Cope M and Delpy D T 1992 The theoretical basis for the determination of optical pathlengths in tissue: temporal and frequency analysis *Phys. Med. Biol.* **37** 1531–60
- Arridge S R, Dehghani H, Schweiger M and Okada E 1999 The finite element model for the propagation of light in scattering media: a direct method for domains with non-scattering regions *Med. Phys.* at press
- Arridge S R and Schweiger M 1998 A gradient-based optimisation scheme for optical tomography *Opt. Express* **2** 213–26
- Arridge S R, Schweiger M, Hiraoka M and Delpy D T 1993 A finite element approach for modeling photon transport in tissue *Med. Phys.* **20** 299–309
- Bassani M, Martelli F, Zaccanti G and Contini D 1997 Independence of the diffusion coefficient from absorption: experimental and numerical evidence *Opt. Lett.* **22** 853–5
- Carlson B G and Lathrop K D 1968 Transport theory *The Method of Discrete Ordinates in Computation Methods in Reactor Physics* ed H Greenspan, C N Kelber and D Okrent (New York: Gordon and Breach) pp 171–270
- Case M C and Zweifel P F 1967 *Linear Transport Theory* (New York: Addison-Wesley)
- Colak S B, Papaioannou D G, Hooft W G, van der Mark M B, Schomberg H, Paasschens J C J, Melissen J B M and van Asten N A A J 1997 Tomographic image reconstruction from optical projections in light-diffusing media *Appl. Opt.* **36** 180–213
- Chandrasekhar R 1950 *Radiation Transfer* (Oxford: Clarendon)
- Dorn O 1998 A transport back-transport method for optical tomography *Inverse Problems* **14** 1107–30
- Dunderstadt J J and Martin W R 1979 *Transport Theory* (New York: Wiley)
- Fantini S, Franceschini M A, Gaida G, Gratton E, Jess H, Mantulin W W, Moesta K T, Schlag P M and Kaschke M 1996 Frequency domain optical mammography: edge effect corrections *Med. Phys.* **23** 149–57

- Firbank M, Arridge S R, Schweiger M and Delpy D T 1996 An investigation of light transport through scattering bodies with non-scattering regions *Phys. Med. Biol.* **41** 767–83
- Groenhuis R A J, Ferwada H A and Ten Bosch J J 1983 Scattering and absorption of turbid materials determined from reflection measurements (parts 1 and 2) *Appl. Opt.* **22** 2456–67
- Hebden J C, Arridge S R and Delpy D T 1997 Optical imaging in medicine: I. Experimental techniques *Phys. Med. Biol.* **42** 825–40
- Hielscher A H and Alcouffe R E 1996 Non-diffusive photon migration in homogenous and heterogenous tissues *Proc. SPIE* **2925** 22–30
- Hielscher A H, Alcouffe R E and Barbour R L 1997 Transport and diffusion calculations on MRI-generated data *Proc. SPIE* **2979** 500–8
- Hielscher A H, Alcouffe R E, Hanson K M and George J S 1996 Comparison of finite difference transport and diffusion calculations for photon migration in homogenous and heterogeneous tissues *Proc. OSA TOPS* **2** 55–9
- Jiang H, Paulsen K D, Osterberg U L, Pogue B W and Patterson M S 1995 Optical image reconstruction using frequency-domain data: simulations and experiments *J. Opt. Soc. Am. A* **13** 431–41
- Nakai T, Nishimura G, Yamamoto K and Tamura M 1997 Expression of optical diffusion coefficient in high-absorption turbid media *Phys. Med. Biol.* **42** 2541–9
- Okada E, Firbank M, Schweiger M, Arridge S R, Cope M and Delpy D T 1997 Theoretical and experimental investigation of near-infrared light propagation in a model of the adult head *Appl. Opt.* **36** 21–31
- Pogue B W, Patterson M S, Jiang H and Paulsen K D 1995 Initial assessment of a simple system for frequency domain diffuse optical tomography *Phys. Med. Biol.* **40** 1709–29
- Schweiger M, Arridge S R and Delpy D T 1993 Application of the finite element method for the forward and inverse problem in optical tomography *J. Math. Imaging Vision* **3** 263–83
- Schweiger M, Arridge S R, Hiraoka M and Delpy D T 1995 The finite element model for the propagation of light in scattering media: boundary and source conditions *Med. Phys.* **22** 1779–92
- Wang Y, Danen R M, Thayer W S, Chance B and Yodh A G 1998 Near-infrared imaging and optical properties of tissue phantoms having curved boundaries and clear layers *Adv. Opt. Imaging Photon Migration OSA TOPS* **21** 142–5